Mobile Telesurgery Platform in Mixed Reality

Literature Review

Team member: Guanhao(Dean) Fu

gfu3@jhu.edu

Mentors:

Dr. Peter Kazanzides

Ehsan Azimi

04/27/2020

Reviewed Literature

El-Gohary, M., & McNames, J. (2012). Shoulder and elbow joint angle tracking with inertial sensors. IEEE Transactions on Biomedical Engineering, 59(9), 2635–2641. https://doi.org/10.1109/TBME.2012.2208750

Introduction

- Project

My project in CIS 2 is to design a system that tracks in real-time human's arm motion, in particular, the position and orientation of human's palm in 3D cartesian space. In specific, I choose to use a 2-IMU system that's strapped on human subjects' upper arm and wrist to capture shoulder, elbow, and wrist angles, and together with the subject arm's D-H parameter, to calculate the position and orientation of the subject's palm.

- Paper Selection

I selected this paper to review because it describes a system that is almost identical to the system my project desires. In addition, it has very good accuracy in regards to shoulder, elbow, and wrist joint angle calculations when compared to a optical tracker, which itself is very accurate.

- Key Contribution and Results

This paper introduces a novel UKF (unscented-Kalman Filter) for estimating human shoulder (3DOF), elbow (1DOF) and wrist (1DOF) joint angles that remains accurate (peak RMS < 9.8 deg) for a long period of time (2min) compared to other similar Kalman Filter based sensor fusion algorithm.
In addition, the correlation coefficient between IMU output and optical tracker output is relatively high: r>0.95, meaning that the system tracks the human arm movement very well.

Background

- IMU

The IMU is a microelectromechanical system that can be mass-manufactured at low cost [3]. It has 3 sensors integrated, which are triaxial gyroscope, triaxial accelerometer, and triaxial magnetometer. The gyroscope outputs angular velocity, the accelerometer outputs linear acceleration, and the magnetometer outputs magnetic field strength. Traditionally, the orientation of the IMU's body-fixed frame can be obtained by integrating the angular velocity output by the gyroscope, however, the noise in the gyroscope accumulates quickly and can result in orientation drift after a short amount of time. As a result, there are various Kalman Filters that fuse the output by gyroscope and accelerometer to reduce z-axis drift, however it is still persistent, although at a slower rate. Other Kalman Filters fuse gyroscope, accelerometer, as well as magnetometer to produce orientation, however, this method is greatly susceptible to magnetic field disturbance that is created by electronic devices which are common nowadays. So in order to use this type of sensor fusion, the environment of the application is rather important, and can oftentimes be counter-intuitive for some applications (surgical applications where magnetic field disturbance cannot be get rid of).

- Human arm joint angles

Human arm consists of 7 Degrees of Freedom (DOF) that are distinguished by shoulder, elbow, and wrist. The shoulder has 3 DOF that are abduction/adduction, flexion/extension, internal/external rotation; the elbow has 2 DOF that are elbow flexion/extension, and forearm supination/pronation; the wrist has 2 DOF which are abduction/adduction, and flexion/extension.

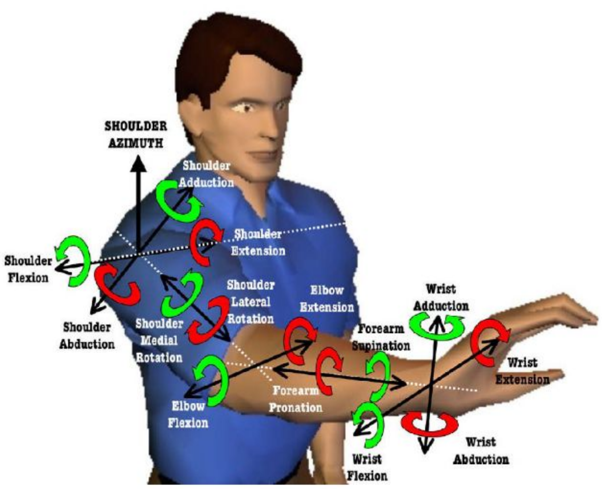

Figure 1. Human arm joint angles [5]

- Denavit–Hartenberg parameters

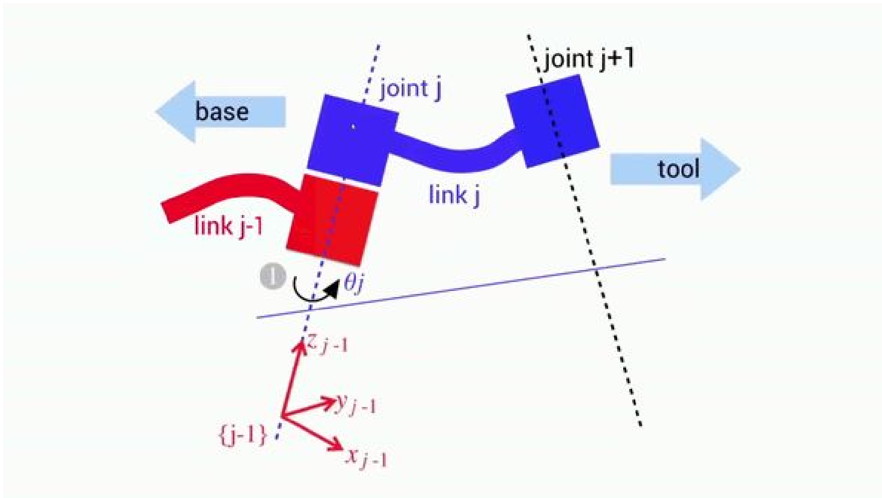

Figure 2. D-H parameter visualization [1]

DH parameters is a convention that describes reference frames of the links of a spatial kinematic chain. It consists of 4 parameters, which are 2 translations and 2 rotations. The sequence of the translations and rotations is: first rotate around z-axis of link j-1 with θ; then translate along z-axis of link j-1 about d; further translate along x-axis of link j-1 about a, which arrives at link j; finally rotate around x-axis with α.

$$ {}^{i-1}A_i = Rot_{z,\theta_i} Trans_{z,d_i} Trans_{x,a_i} Rot_{x,\alpha_i} $$

Figure 3. D-H parameters [2]

Theory

- Human arm kinematics (D-H parameters)

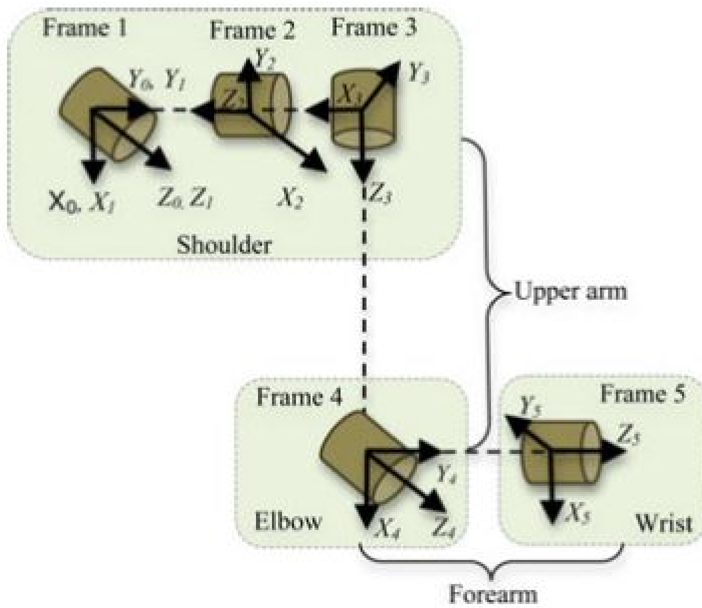

Figure 4. Human arm link model [4]

Figure 4 shows the kinematics diagram of the arm model. Frames 1 through 3 represent shoulder flexion/extension, abduction/adduction and internal/external rotation, respectively. Frames 4 through 5 represent the elbow flexion/extension and forearm pronation/supination.

DENAVIT–HARTENBERG PARAMETERS FOR THE ARM MODEL

Frame	α_{i-1}	a_{i-1}	d_i	θ_i
1	0	0	0	θ_1
2	$\pi/2$	0	0	$\theta_2 + \pi/2$
3	$\pi/2$	0	l_u	$\theta_3 + \pi/2$
4	$\pi/2$	0	0	$\theta_4 + \pi/2$
5	$-\pi/2$	0	l_f	θ_5

Figure 5. Human arm D-H parameter [4]

Figure 5 shows the D-H parameters of the human arm, according to the description of D-H parameters in the *Background* section, the (θ, d, a, α) are of the same convention. αi-1 is the angle of rotation to make the two coordinate system coincide, lu is the length of the upper arm, lf is the length of the forearm, and θi are the angles of each joint frame.

Experimental setup

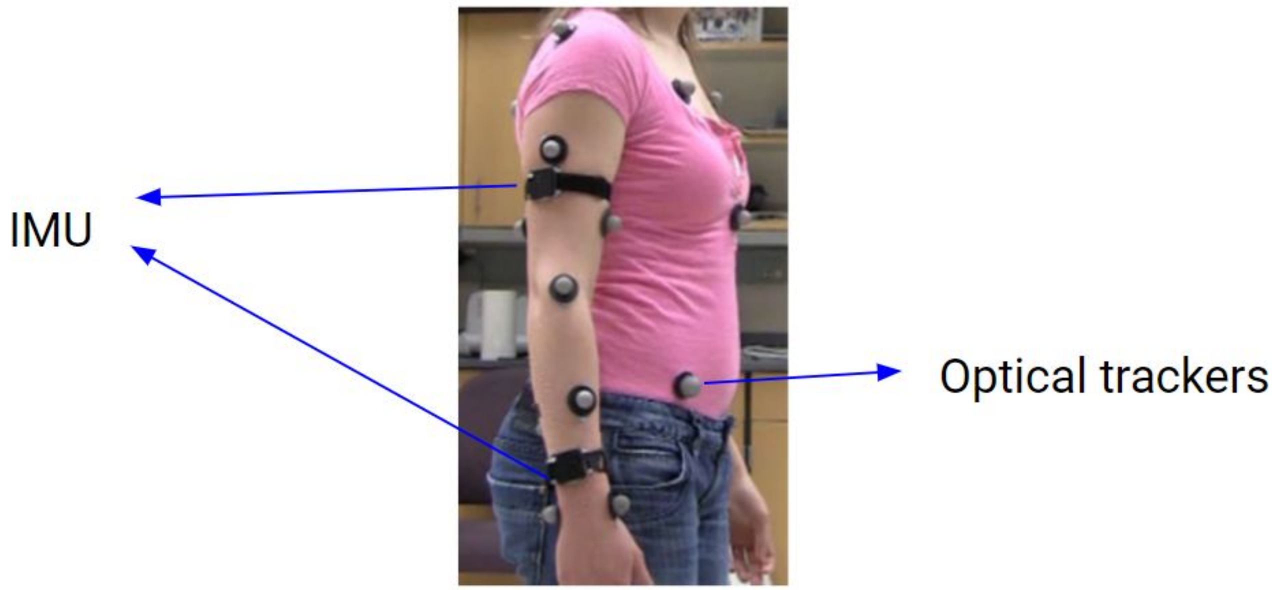

Figure 6. Reflective markers and Opal inertial sensors (APDM, Inc.) placement on the arm of one of the subjects.[4]

Kalman Filter

The paper uses a Unscented-Kalman Filter (UKF) to reduce the IMU drift that occurs overtime. Specifically, the state-transition model and observation model are both non-linear.

$$x(n+1) = f_n\left[x(n), u(n)\right]$$
$$y(n) = h_n\left[x(n), v(n)\right]$$

Figure 7. KF generic equation [4]

$$\theta_i(n+1) = \theta_i(n) + T_s\dot{\theta}_i(n) + \frac{1}{2}T_s^2\ddot{\theta}_i(n)$$
$$\dot{\theta}_i(n+1) = \dot{\theta}_i(n) + T_s\ddot{\theta}_i(n)$$
$$\ddot{\theta}_i(n+1) = \alpha\ddot{\theta}_i(n) + u_{\ddot{\theta}_i}(n)$$

where $i = \{1, \ldots, 5\}$ of the five angles, $\theta_i(n)$ is the ith angle at time n, $\dot{\theta}_i$ is the angular velocity, $\ddot{\theta}_i$ is the angular acceleration, $u_{\ddot{\theta}_i}(n)$ is a white noise process with zero mean, α is a process model parameter, and $T_s = 1/f_s$ is the sampling period.

Figure 8. KF state transition model [4]

$$\begin{aligned}
\dot{\omega}_z &= \dot{\theta}_3 + \dot{\theta}_1 s\theta_2 \\
\dot{\omega}_x &= \dot{\theta}_1 c\theta_2 s\theta_3 - \dot{\theta}_2 c\theta_3 \\
\dot{\omega}_y &= \dot{\theta}_1 c\theta_2 c\theta_3 + \dot{\theta}_2 s\theta_3 \\
\dot{v}_x &= -l_u[\dot{\theta}_1^2 c\theta_2^2 + \dot{\theta}_2^2] - gc\theta_1 c\theta_2 \\
\dot{v}_y &= l_u[c\theta_2 s\theta_2 s\theta_3 \dot{\theta}_1^2 - 2\dot{\theta}_2 c\theta_3 s\theta_2 \dot{\theta}_1 + \ddot{\theta}_2 s\theta_3 + \ddot{\theta}_1 c\theta_2 c\theta_3] \\
&\quad + g[c\theta_3 s\theta_1 + c\theta_1 s\theta_2 s\theta_3] \\
\dot{v}_z &= l_u[c\theta_2 c\theta_3 s\theta_2 \dot{\theta}_1^2 + 2\dot{\theta}_2 s\theta_2 s\theta_3 \dot{\theta}_1 + \ddot{\theta}_2 c\theta_3 - \ddot{\theta}_1 c\theta_2 s\theta_3] \\
&\quad - g[s\theta_1 s\theta_3 + c\theta_1 c\theta_3 s\theta_2]
\end{aligned}$$

Figure 9. KF observation model [4]

ω is the angular velocity outputted by gyroscope, and v-dot is the linear acceleration outputted by accelerometer.
Note that the link-length (lu) is present in the observation model, which, I suspect, is what makes this paper's UKF unique and "accurate".

Results

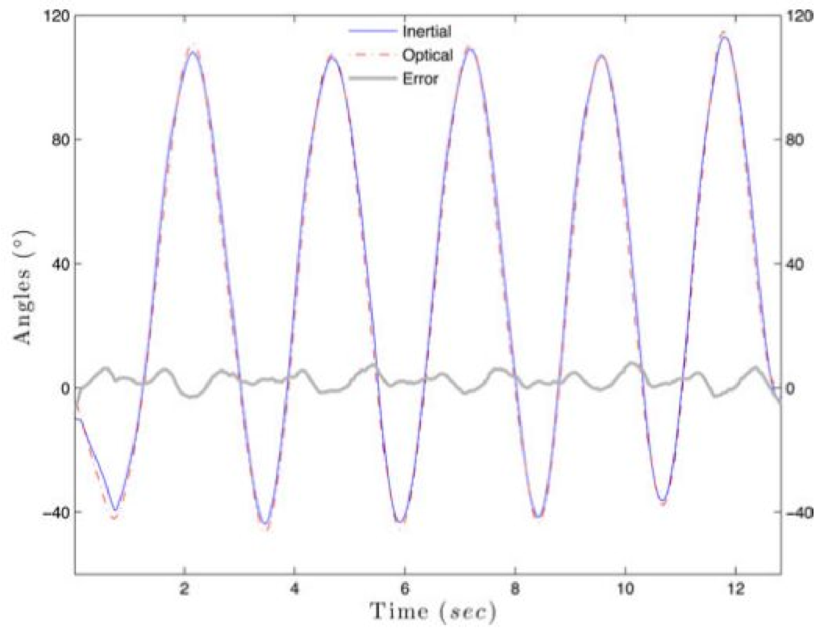

Figure 10. shoulder angles - abduction/adduction [4]

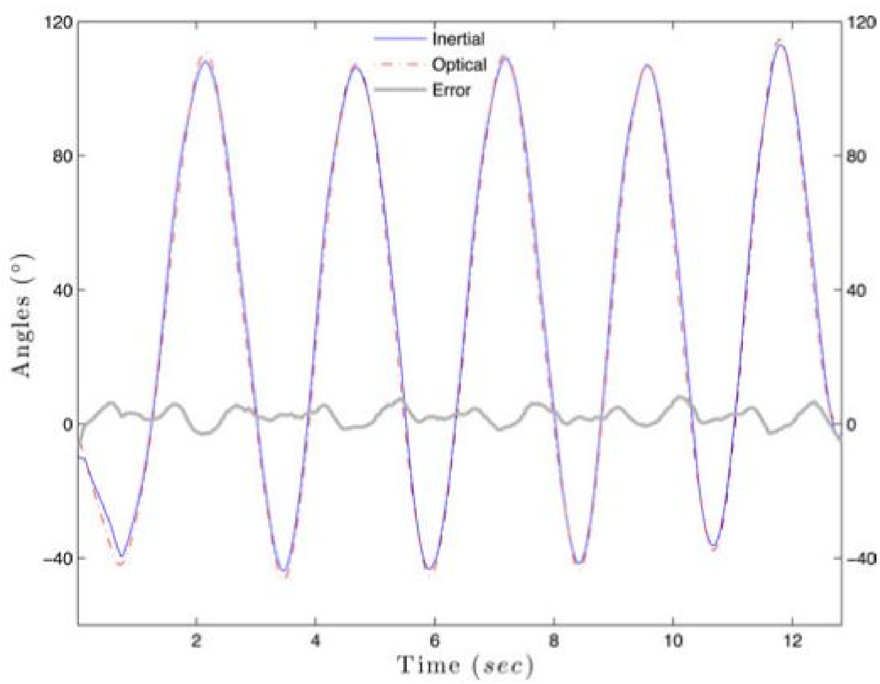

Figure 11. shoulder angles - flexion/extension [4]

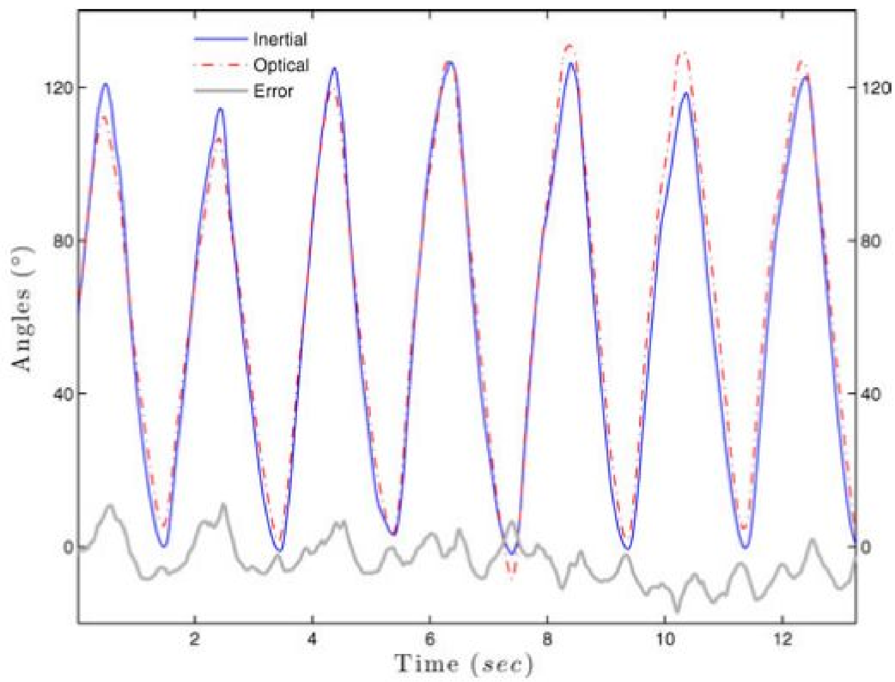

Figure 12. forearm supination/pronation [4]

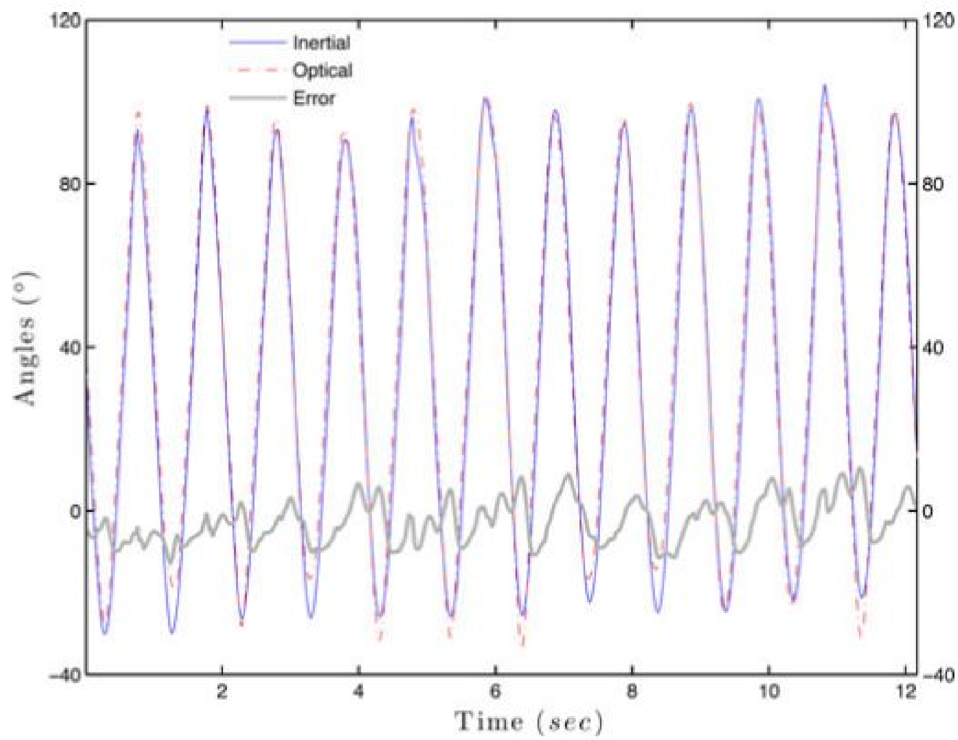

Figure 13. elbow flexion/extension [4]

As can be seen in the legend of these 4 plots, the correlation between inertial result and optical result are relatively high, which the paper indicates as follows:

TABLE II
AVERAGE CORRELATION r, RMSE, AND PEAK-TO-PEAK ERROR BETWEEN OPTICAL AND INERTIAL ANGLES OF SHOULDER AND ELBOW

Task	r	RMSE(°)	Peak Error(°)
Elbow Flexion/Extension	0.98	6.5	9.8
Forearm Supination/Pronation	0.95	5.5	7.8
Shoulder Flexion/Extension	0.98	5.5	7.9
Shoulder Abduction/Adduction	0.99	4.4	8.1

TABLE III
AVERAGE CORRELATION r AND RMSE BETWEEN OPTICAL AND INERTIAL ANGLES OF SHOULDER AND ELBOW

Task	r	RMSE(°)	Peak Error(°)
Touching nose	0.94	6.5	9.8
Reaching for a doorknob	0.95	5.5	8.8

Assessment

- Pros

1. The result shows relatively high correlation between optical and inertial angles of joint angles of human arms.
2. The "accurate" period of time of this paper (2min) is longer than other relevant works.
3. Detailed Kalman Filter model for readers' implementation.

- Cons

1. No result for shoulder internal/external rotation data, only synthetic data, and did not explain why it is missing.
2. No explanation of why the IMU's internal Kalman Filter is insufficient and whether their UKF is superior, and what problem does it solve compared to the internal KF.

- Relevance to project

1. The paper presents a real-time human arm joint angle tracking system that is generalized enough to track other limbs if desired.
2. The assumption is the same as my project: the human subject's trunk must remain perpendicular to the ground. This ensures that the shoulder base frame has the same z-axis as the body frame, which is the same as the IMU frame's z-axis. This is important because the IMU's z-axis is always perpendicular to the ground due to earth's acceleration g.
3. IMU placement is a good starting point for my project.
4. Invokes further study: does external Kalman Filter really necessary to reduce IMU drift when there is internal KF in the IMUs in a human-in-the-loop application?

Conclusion

This paper is highly relevant to my project given that we both use a 2-IMU system to track human arm joint angles. Furthermore, this paper has a solid summary of what others had done in the past with regards to sensor fusion of IMUs. Most importantly, this paper summarizes and provides the D-H parameter for the human arm that I could use or adapt in my demonstration.

Reference

1. D-H parameters https://robotacademy.net.au/lesson/denavit-hartenberg-notation/
2. D-H paratmeters http://www.aeromech.usyd.edu.au/MTRX4700/Course_Documents/material/lectures/L2_Kinematics_Dynamics_2013.pdf
3. IMU lecture https://stanford.edu/class/ee267/notes/ee267_notes_imu.pdf
4. El-Gohary, M., & McNames, J. (2012). Shoulder and elbow joint angle tracking with inertial sensors. IEEE Transactions on Biomedical Engineering, 59(9), 2635–2641. https://doi.org/10.1109/TBME.2012.2208750
5. Naidu, D., Stopforth, R., Bright, G., & Davrajh, S. (2011). A 7 DOF exoskeleton arm: Shoulder, elbow, wrist and hand mechanism for assistance to upper limb disabled individuals. IEEE AFRICON Conference, (September), 1–6. https://doi.org/10.1109/AFRCON.2011.6072065